Boundary-Layer Meteorol (2007) 122:205–216
DOI 10.1007/s10546-006-9105-1

ORIGINAL PAPER

Simplified expressions for adjusting higher-order turbulent statistics obtained from open path gas analyzers

M. Detto · G. G. Katul

Received: 12 December 2005 / Accepted: 26 June 2006 /
Published online: 21 October 2006

Abstract When density fluctuations of scalars such as CO_2 are measured with open-path gas analyzers, the measured vertical turbulent flux must be adjusted to take into account fluctuations induced by 'external effects' such as temperature and water vapour. These adjustments are needed to separate the effects of surface fluxes responsible for 'natural' fluctuations in CO_2 concentration from these external effects. Analogous to vertical fluxes, simplified expressions for separating the 'external effects' from higher-order scalar density turbulence statistics are derived. The level of complexity in terms of input to these expressions are analogous to that of the Webb–Pearman–Leuning (WPL), and are shown to be consistent with the conservation of dry air. It is demonstrated that both higher-order turbulent moments such as the scalar variances, the mixed velocity-scalar covariances, and the two-scalar covariance require significant adjustments due to 'external effects'. The impact of these adjustments on the turbulent CO_2 spectra, probability density function, and dimensionless similarity functions derived from flux-variance relationships are also discussed.

Keywords Carbon flux · Flux correction · Higher order statistics · Open path gas analyzer

M. Detto (✉)
Dipartimento di Ingegneria Idraulica, Ambientale e del Rilevamento, Politecnico di Milano, P.zza L. Da Vinci 32, Italy
e-mail: matteo.detto@polimi.it

G. G. Katul
Nicholas School of the Environment and Earth Sciences, Box 90328, Duke University, Durham, NC, USA

Department of Civil and Environmental Engineering, Pratt School of Engineering, Duke University, Durham, NC, USA

1 Introduction

Continuous long-term eddy-covariance flux measurements of CO_2 exchange between canopies and the atmospheres are now possible primarily because of the availability of open-path gas analyzers (e.g. CO_2/H_2O infrared gas analyzer, Li-cor7500, Lincoln, Nebraska). Such flux measurements are now proliferating worldwide as part of a long-term global CO_2 flux monitoring initiative from terrestrial biomes known as FluxNet (Baldocchi et al. 2001). Concomitant with the long-term flux measurements, a surge in micrometeorological field studies of biosphere—atmosphere CO_2 exchange is also developing driven primarily by applications ranging from the use of higher-order closure models to compute CO_2 transport (Siqueira et al. 2000), to CO_2 advection on complex terrain (Feigenwinter et al. 2004; Staebler and Fitzjarrald 2004; Aubinet et al. 2005), to low-frequency spectral similarity analysis between water vapour and CO_2. These studies are now motivating detailed analysis of measured higher-order turbulence statistics derived from open-path gas analyzers (e.g. mixed scalar-velocity moments).

For scalars such as CO_2, the measured vertical flux from eddy-covariance systems is adjusted by the so-called Webb–Pearman–Leuning (WPL) correction (Webb et al. 1980) because fluctuations in temperature and water vapour impact the linkages between these measured fluxes and desired scalar sources and sinks from ecosystems. The WPL correction and various revisions received significant theoretical attention recently (Fuehrer and Friehe 2002; Massman and Lee 2002; Liebethal and Foken 2003; Liu 2005) because long-term CO_2 fluxes are now being conducted over a broad range of climatic conditions for which sensible heat and latent heat fluxes vary appreciably. Minor corrections induced by WPL may even shift the sign of the CO_2 flux in some ecosystems.

Besides vertical fluxes of CO_2, other second-order moments are being measured and often employed in micrometeorological applications such as, (1) evaluating components of the turbulent CO_2 flux budget for testing higher-order turbulent closure models (e.g. Juang et al. 2006), (2) assessing second-moment similarity relationships for flux-variance CO_2 calculations, now proposed as a plausible gap-filling method (Choi et al. 2004), (3) comparing similarity in turbulent transport efficiencies between CO_2 and other scalars such as heat and water vapour often used to inspect similarities in sources and sinks at the ground, and perhaps 'de-code' the role of entrainment processes from the top of the mixed layer (de Arellano et al. 2004), and (4) conducting drainage or CO_2 advection studies on sloping terrain that often necessitate measurements of longitudinal and lateral CO_2 fluxes (Feigenwinter et al. 2004; Staebler and Fitzjarrald 2004; Aubinet et al. 2005). Hence, as in WPL, corrections to CO_2 variances, horizontal and lateral turbulent fluxes, and the covariance between temperature and CO_2 as well as covariances among various tracers themselves (e.g. water vapour and CO_2) are clearly needed. To date, an equivalent WPL correction for these higher-order statistics has not been derived, the subject of this study. Our intent is not to revise WPL or propose new formulations to the vertical flux of CO_2; rather, we seek simplified expressions to link higher-order statistics measured from open-path gas analyzers and sonic anemometers with general turbulent transport processes in the atmosphere.

2 Theory

The density fluctuations of any scalar c ($\rho_c' = \rho_c - \bar{\rho}_c$, where the overbar indicates Reynolds averaging and primed quantities are fluctuations) such as CO_2 in the atmosphere (expressed as moles of c per unit volume of air) can be decomposed into two contributions: one due to the 'natural' fluctuations by the transport phenomena such as turbulence ($\rho_{c,\mathrm{nat}}$) and the other due to fluctuations in external conditions ($\rho_{c,\mathrm{ext}}'$) mainly due to changes in air temperature (T) and water vapour density (ρ_q). In micrometeorological applications, separating these 'external' fluctuations from the measured density fluctuations is needed when linkages between sources and sinks of scalar c at the ground and turbulent fluxes in the atmosphere is investigated. Hence, the instantaneous scalar density and its variations can be expressed as

$$\rho_c = \rho_{c,\mathrm{nat}} + \rho_{c,\mathrm{ext}}', \tag{1a}$$

$$\rho_c' = \rho_{c,\mathrm{nat}}' + \rho_{c,\mathrm{ext}}'. \tag{1b}$$

To link $\rho_{c,\mathrm{ext}}$ to changes in T and ρ_q, we consider a simplified set-up comprising of a balloon of finite volume V that has a fixed number of molecules of scalar c (n_c) and dry air (n_a). Because we seek an expression for $\rho_{c,\mathrm{ext}}'$, the balloon is not permitted to exchange scalars through its sides. Increasing the balloon temperature T isobarically produces a volume expansion described by the ideal gas law $V = n_\mathrm{t}TR/P$, where P is the total pressure, R is the universal gas constant, and n_t is the total number of molecules ($n_\mathrm{t} = n_a + n_q + n_c$, where n_q are the water vapour molecules). This volume expansion logically results in a decrease in $\rho_c (= n_c/V)$. Likewise, if additional water vapour molecules are forced into the balloon isobarically at the same T, n_t must increase resulting in a volume expansion and concomitant reduction in ρ_c. Naturally, a decrease in T or reductions in n_q will have the opposite effect on ρ_c.

In the absence of the injection or removal of molecules of dry air (i.e. mass of dry air is preserved) and c, n_a/n_c is the only constant throughout this experiment. Again, we emphasize that the reason n_c is constant here is due to the fact that we are interested in deriving expressions for $\rho_{c,\mathrm{ext}}'$. Hence, with a constant n_a/n_c, it is convenient to express

$$\rho_c = \frac{n_c}{V} = \frac{n_c}{n_a}\frac{n_a}{V} = \frac{n_c}{n_a}\rho_a, \tag{2}$$

and

$$\rho_{c,\mathrm{ext}}' = \frac{n_c}{n_a}\rho_a', \tag{3}$$

where $n_c/n_a = n_c\overline{V^{-1}}/n_a\overline{V^{-1}} = \bar{\rho}_c/\bar{\rho}_a$.

Following Webb et al. (1980) the fluctuation of dry air can be expressed as a function of temperature and water vapour fluctuations by

$$\rho_a' \approx -\mu\rho_q' - \bar{\rho}_a(1+\mu\sigma)\frac{T'}{\bar{T}} \tag{4}$$

where $\mu = m_a/m_q$ is the ratio between the molecular mass of dry air (m_a) and water vapour (m_q) and $\sigma = \bar{\rho}_q/\bar{\rho}_a$. Combining Eqs. 1–4, we obtain an explicit expression that relates natural fluctuation of any scalar to its measured value and to fluctuations of air temperature and water vapour:

$$\rho'_{c,\mathrm{nat}} = \rho'_c + \left(\mu\frac{\bar{\rho}_c}{\bar{\rho}_a}\rho'_q + \bar{\rho}_c(1+\mu\sigma)\frac{T'}{\bar{T}}\right), \tag{5a}$$

$$\rho'_{c,\mathrm{nat}} = \rho'_c - \rho'_{\mathrm{ext}}. \tag{5b}$$

From Eq. 1, note that $\bar{\rho}_{c,\mathrm{nat}} = \bar{\rho}_c$ because $\overline{\rho'_{\mathrm{ext}}} = 0$ and these external effects do not alter the mean CO_2 density. It is now straightforward to derive from Eq. 5 all the higher-order statistics of $\rho'_{c,\mathrm{nat}}$ from ρ'_c. For instance, multiplying Eq. 5 by the turbulent vertical velocity w' and applying Reynolds averaging we obtain

$$\overline{w'\rho'_{c\mathrm{nat}}} = \overline{w'\rho'_c} + \mu\frac{\bar{\rho}_c}{\bar{\rho}_a}\overline{w'\rho'_q} + \bar{\rho}_c(1+\mu\sigma)\frac{\overline{w'T'}}{\bar{T}}. \tag{6}$$

Equation 6 is identical to Webb et al. (1980) who derived this result using the zero dry air flux constraint. Similarly, all the second-order statistics can be derived and are given by:

$$\overline{u'_i\rho'_{c\mathrm{nat}}} = \overline{\rho'_c} + \mu\frac{\bar{\rho}_c}{\bar{\rho}_a}\overline{u'_i\rho'_q} + \bar{\rho}_c(1+\mu\sigma)\frac{\overline{u'_iT'}}{\bar{T}} \tag{7}$$

where u'_i $(= u', v', w')$ are the turbulent velocity fluctuations in direction x_i $(= x, y, z$, with x being the longitudinal, y being the lateral, and z being the vertical coordinates, respectively), and

$$\overline{T'\rho'_{c\mathrm{nat}}} = \overline{T'\rho'_c} + \mu\frac{\bar{\rho}_c}{\bar{\rho}_a}\overline{T'\rho'_q} + \bar{\rho}_c(1+\mu\sigma)\frac{\overline{T'^2}}{\bar{T}}, \tag{8}$$

$$\begin{aligned}\overline{\rho'^2_{c\mathrm{nat}}} = {} & \overline{\rho'^2_c} + 2\mu\frac{\bar{\rho}_c}{\bar{\rho}_a}\overline{\rho'_q\rho'_c} + 2\bar{\rho}_c(1+\mu\sigma)\frac{\overline{T'\rho'_c}}{\bar{T}} \\ & + \mu^2\frac{\bar{\rho}_c^2}{\bar{\rho}_a^2}\overline{\rho'^2_q} + \bar{\rho}_c^2(1+\mu\sigma)^2\frac{\overline{T'^2}}{\bar{T}^2} \\ & + 2\frac{\bar{\rho}_c^2}{\bar{\rho}_a}\mu(1+\mu\sigma)\frac{\overline{T'\rho'_q}}{\bar{T}}.\end{aligned} \tag{9}$$

The covariance between two scalars $\overline{\rho'_{c_1}\rho'_{c_2\mathrm{nat}}}$ is also given by

$$\begin{aligned}\overline{\rho'_{c_1}\rho'_{c_2\mathrm{nat}}} = {} & \overline{\rho'_{c_1}\rho'_{c_2}} + \frac{\mu}{\bar{\rho}_a}\left(\bar{\rho}_{c_2}\overline{\rho'_q\rho'_{c_1}} + \bar{\rho}_{c_1}\overline{\rho'_q\rho'_{c_2}}\right) \\ & + (1+\mu\sigma)\left(\bar{\rho}_{c_1}\frac{\overline{T'\rho'_{c_2}}}{\bar{T}} + \bar{\rho}_{c_2}\frac{\overline{T'\rho'_{c_1}}}{\bar{T}}\right) \\ & + \mu^2\frac{\bar{\rho}_{c_1}\bar{\rho}_{c_2}}{\bar{\rho}_a^2}\overline{\rho'^2_q} + 2\mu\frac{\bar{\rho}_{c_1}\bar{\rho}_{c_2}}{\bar{\rho}_a}(1+\mu\sigma)\frac{\overline{T'\rho'_q}}{\bar{T}} \\ & + \bar{\rho}_{c_1}\bar{\rho}_{c_2}(1+\mu\sigma)^2\frac{\overline{T'^2}}{\bar{T}^2}.\end{aligned} \tag{10}$$

All terms that appear on the right-hand side of Eqs. 6–10 are variances or covariances that can be independently measured by infrared gas analyzers and sonic anemometers. For consistency with previous studies, the difference between 'natural' and 'measured' fluctuations is hereafter referred to as a 'correction' though this term is not the most accurate nomenclature.

3 Method

We used high frequency scalar density and velocity measurements collected at 2.8 m above a grass-covered surface within the Blackwood division of the Duke Forest near Durham, North Carolina, U.S.A. to assess the magnitude of these corrections. The site characteristics are described elsewhere (Novick et al. 2004). The scalar density (in mmoles m^{-3}) was acquired at 10 Hz using a Li-cor7500 (Licor, Lincoln, Nebraska) open-path infrared gas analyzer and the velocity measurements were acquired using a CSAT3 (Campbell Scientific Inc, Logan, Utah) triaxial sonic anemometer. The separation distance between the CSAT3 and the Li-cor7500 was 0.1 m and comparable to the averaging path length of the CSAT3. The experiment commenced on October 2 and was terminated on November 15, 2005. The 10 Hz data were then decomposed into half-hourly runs and all the statistical analyses were conducted on each run. We excluded runs when (1) the sensible heat flux did not exceed 50 W m^{-2}, (2) the WPL 'corrected' CO_2 flux was not within a reasonable range (2 to -15 μmol m^{-2} s^{-1}), and (3) when the instruments were wet during or immediately following rain. Some 412 runs satisfied these three criteria. The ensemble averaged diurnal variations of the energy fluxes relevant to the calculations of the density corrections and the CO_2 fluxes (corrected and uncorrected) are shown in Fig. 1 for reference.

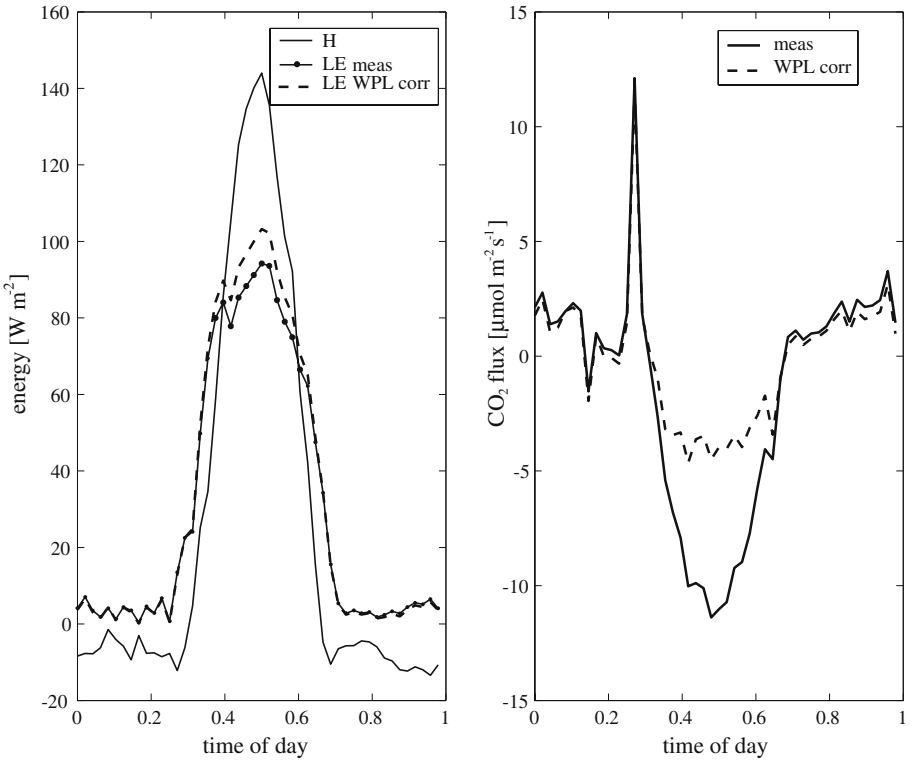

Fig. 1 The diurnal variation of the fluxes for energy (left panel) and net ecosystem CO_2 exchange (right panel) ensemble-averaged over the 47-day experiment period (October 2 – November 17, 2005). For the latent heat and CO_2 fluxes, the WPL corrected values are also shown for reference. Time is in fractions of a day starting at midnight

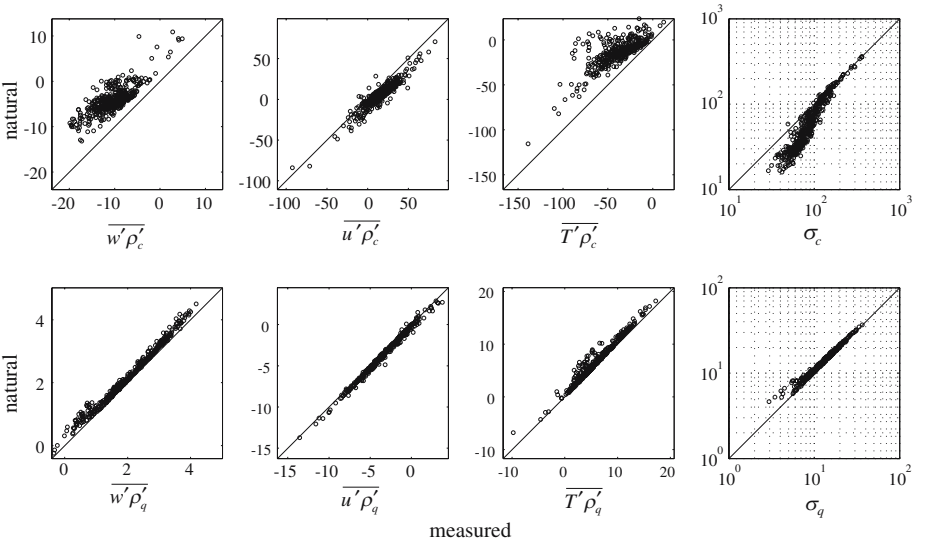

Fig. 2 The comparison between measured (abscissa) and natural (ordinate) co-variances and variances for CO_2 (top panels) and water vapour (bottom panels). The regression statistics are reported in Table 1 along with the units

Table 1 Comparison between the 'measured' (abscissa) and the 'natural' (ordinate) flow variables via linear regression analysis. The slope (a), intercept (b), coefficient of determination (R^2), and the root-mean-squared error (RSE) are shown for all variables

Variable	unit	a	b	R^2	RSE
$\overline{w'\rho'_c}$	[μmol m^{-2} s^{-1}]	0.68	2.94	0.68	6.67
$\overline{u'\rho'_c}$	[μmol m^{-2} s^{-1}]	0.83	−6.56	0.87	10.99
$\overline{T'\rho'_c}$	[K μmol m^{-3}]	0.57	8.89	0.59	28.14
σ_c	[μmol m^{-3}]	1.11	−33.47	0.95	26.35
$\overline{w'\rho'_q}$	[mmol m^{-2} s^{-1}]	0.99	0.20	0.99	0.21
$\overline{u'\rho'_q}$	[mmol m^{-2} s^{-1}]	1.02	−0.21	0.99	0.35
$\overline{T'\rho'_q}$	[K mmol m^{-3}]	1.01	0.70	0.96	1.02
σ_q	[mmol m^{-3}]	1.00	0.75	0.99	0.93
R_{wc}	–	1.04	0.11	0.65	0.13
R_{Tc}	–	1.04	0.30	0.70	0.33
R_{cq}	–	0.99	0.29	0.83	0.34
R_{wq}	–	0.88	0.06	0.96	0.03
R_{Tq}	–	0.88	0.12	0.97	0.06
ϕ_c	–	2.67	−2.49	0.82	3.62
ϕ_q	–	0.63	−0.71	0.90	0.61
ψ_{1c}	–	1.93	−1.41	0.83	2.03
ψ_{1q}	–	0.70	0.48	0.93	0.72

4 Results and discussion

We first show the magnitude of the corrections to $\overline{u'_i\rho'_c}$ ($i = 1,\ 3$), $\overline{\rho'^2_c}$ and $\overline{T'\rho'_c}$ from Eqs. 7–10 in Fig. 2 using the half-hourly statistics. We found that for CO_2, all the corrections are significant and are comparable to what was derived for the vertical flux (see Table 1 for regression analysis). However, for water vapour, these corrections are

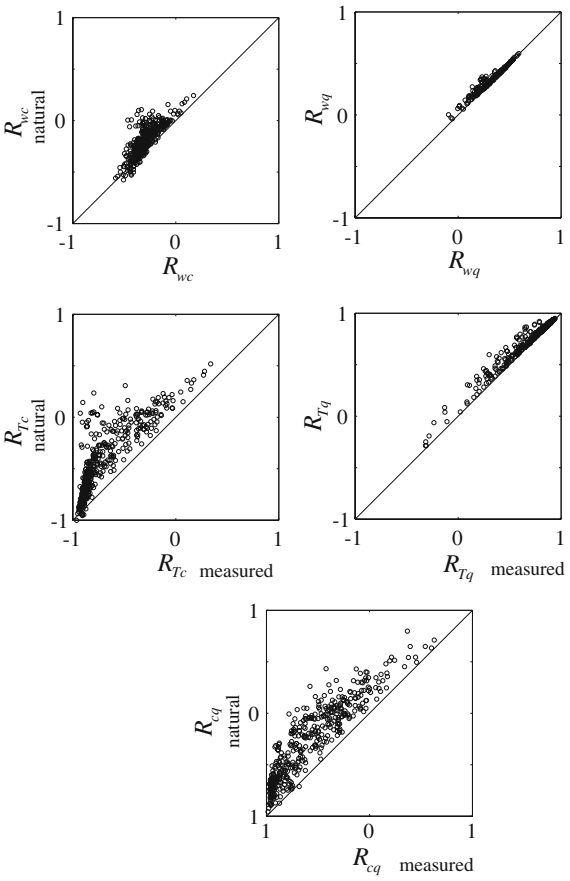

Fig. 3 Same as Fig. 2 but for the correlation coefficients (R_{xy} is the correlation coefficient between variables x and y)

minor (compared to CO_2) but not entirely negligible (see the intercept and root-mean squared error in Table 1).

As earlier stated, similarity between heat, water vapour, and CO_2, as well as modelling higher-order scalar statistics is receiving significant attention within the micrometeorological community (Moriwaki and Kanda 2005; Scanlon and Albertson 2001; Katul et al. 1998). We show the impact of these corrections directly on 'non-dimensional' quantities such as similarity functions or transport efficiencies. Figure 3 presents a comparison between the transport efficiencies and correlation coefficients among the scalars. It is clear that even dimensionless quantities such as R_{Tc} and R_{wc} must be corrected when used in assessing similarity in turbulent diffusivities or turbulent transport efficiencies (here R_{xy} is the correlation coefficient between variables x and y). As before, the magnitude of these corrections to water vapour statistics is minor but not negligible (Fig. 3, Table 1).

The dimensionless quantity $\phi_c(z/L)$, determined from $\frac{\sigma_c}{c_*}$(where $\sigma_c^2 = \overline{\rho_c'^2}$ and $c_* = \overline{w'\rho_c'}/u_*$ and L is the Obukhov length), is often used in assessing flux-variance models and also requires adjustments (Fig. 4). Unadjusted $\phi_c(z/L)$ (i.e. concentration fluctuations taken directly from the raw time series of the gas analyzer) may falsely give the impression that flux-variance similarity theory functions agree well with measurements. This 'false' agreement is attributed to the fact that heat is known to follow

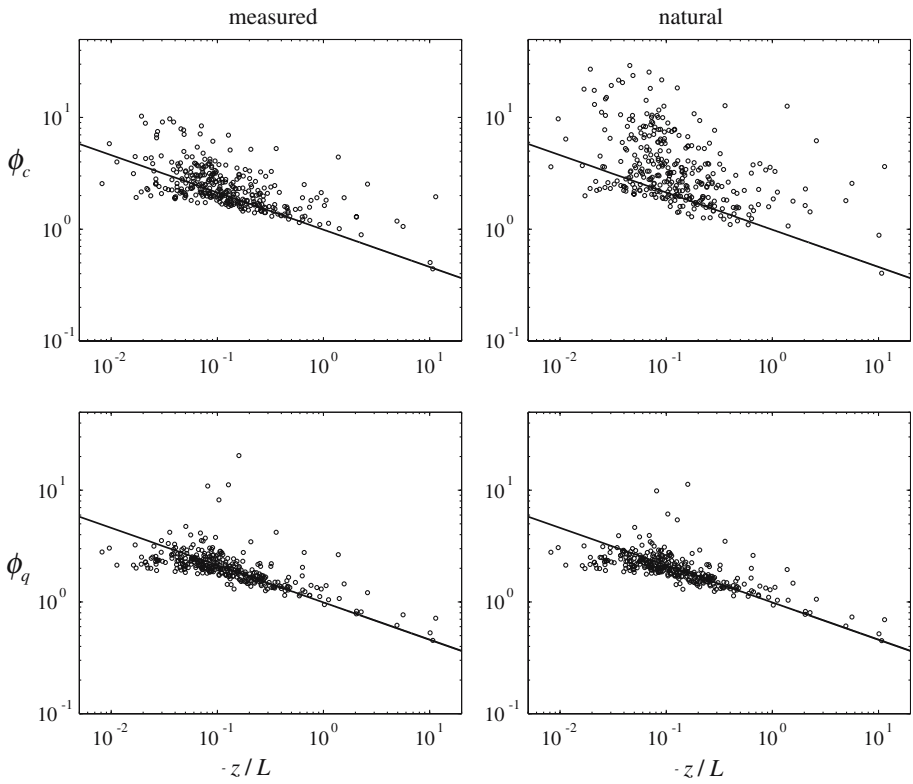

Fig. 4 The variation of flux-variance relationships as a function of the atmospheric stability parameter (z/L) for CO_2(ϕ_c in top panels) and water vapour (ϕ_q in bottom panels). The regression statistics are reported in Table 1. The solid line represents $\phi(z/L) = 0.99\,(-z/L)^{-1/3}$ derived from a homogeneous surface

flux-variance similarity theory better than other scalars, as demonstrated at this particular grass site in Katul et al. (1995), and part of the measured CO_2 concentration fluctuations are attributed to external temperature effects thereby promoting strong correlations between CO_2 and temperature (see also R_{Tc} in Fig. 3).

However, the dimensionless quantity $\psi_{1c} = \overline{u'c'}/\overline{w'c'}$ is more robust to these corrections because the flux biases in the numerator and the denominator are comparable and act in the same direction (see Figs. 4 and 5). Notwithstanding this cancellation, the corrected ψ_{1c} appears more scattered when compared to ψ_{1q}, consistent with previous results about the significant role of these corrections to CO_2 when compared with water vapour.

To explore how these corrections alter the large CO_2 turbulent excursions, we compared a sample probability density function (PDF) of the measured and 'natural' (i.e. evaluated from Eq. 5 using the high frequency time series fluctuations collected under high sensible heat flux conditions). Given that the variances were shown to differ in Fig. 2, we chose to normalize the two series by their respective standard deviations. This normalization ensures that all the differences amongst the two PDFs can be attributable to the impact of temperature and water vapour fluctuations on the higher-order concentration statistics. We found from Fig. 6 that the 'natural' PDF shows a reduced

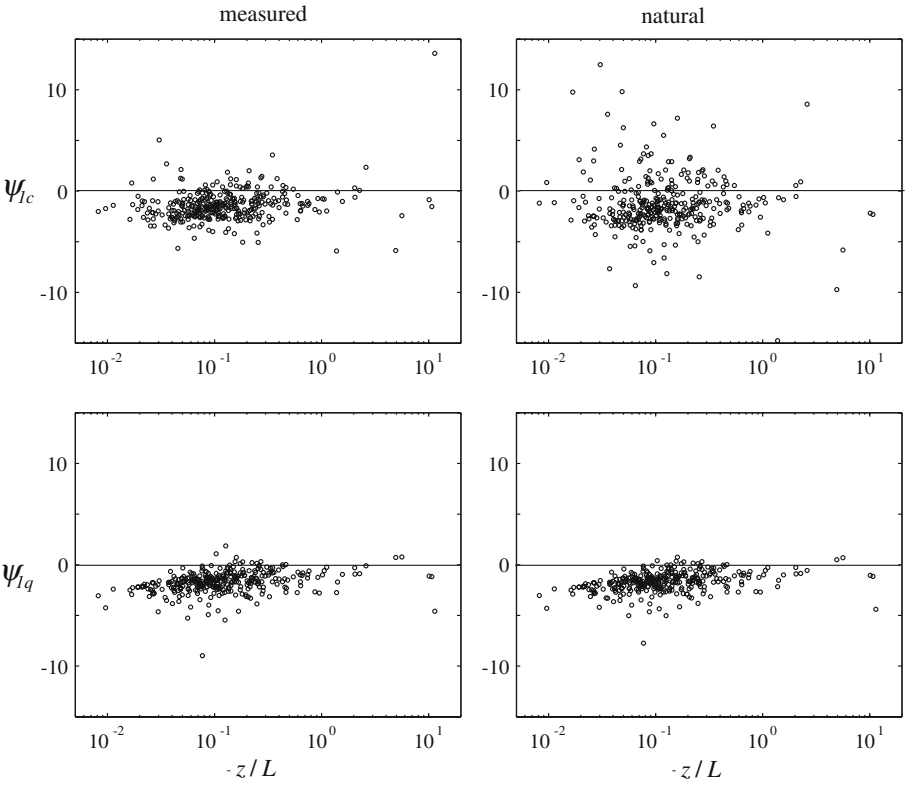

Fig. 5 Same as Fig. 4 but for $\psi_{1c}\left(=\overline{u'c'}/\overline{w'c'}\right)$ (top panel) and $\psi_{1q}\left(=\overline{u'q'}/\overline{w'q'}\right)$(bottom panel)

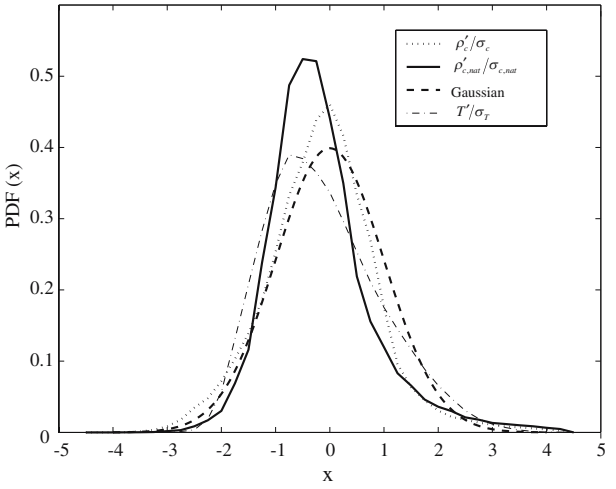

Fig. 6 Probability density functions of the normalized fluctuations of CO_2 'measured' and 'natural' between 1140 and 1230 local time on November 29, 2005. The mean WPL net ecosystem CO_2 flux was -5.7 [μmol m^{-2} s^{-1}], the sensible heat flux was 225.9 [W m^{-2} s^{-1}], and the latent heat flux was 120.1 [W m^{-2} s^{-1}]. For reference, a zero mean unit variance Gaussian distribution PDF along with the PDF of the normalized temperature fluctuations is also shown

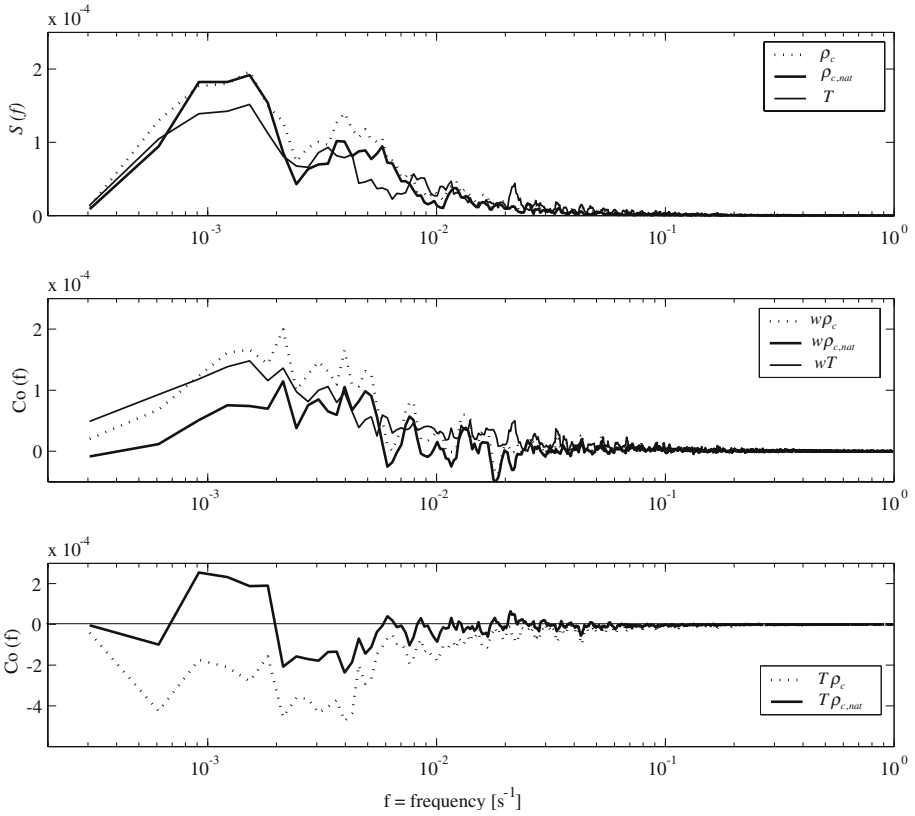

Fig. 7 *Top panel*: The power spectra of CO_2 'measured' and 'natural'. *Middle panel*: the cospectra between vertical velocity and CO_2. *Bottom Panel*: the cospectra between temperature and CO_2, for the same period as Fig. 6. For reference the spectra of temperature (divide by 50 for scale display convenience) and the cospectra between vertical velocity and temperature (divide by 10 for scale display convenience) are also presented

negative tail and a shift in the mode towards negative states. The reduction in the negative tails is not surprising because the large positive temperature excursions are co-located in time with the large negative CO_2 excursions (during daytime, the PDF of T is positively skewed as shown in Fig. 6).

We explore next the spectral interactions between natural and measured CO_2 concentration fluctuations, vertical velocity, and temperature by computing the relevant spectra and cospectra. From Fig. 7, it is clear that much of the intensity of temperature fluctuations resides in time scales comparable to 100–1000 s thereby explaining why the difference in the power spectra of the natural and measured CO_2 concentrations resides at these low-frequency scales. Similarly, the cospectral CO_2 vertical flux adjustments are largest at these low-frequency scales.

To quantify at what time scales temperature and CO_2 interact, so as to assess the time scales at which externals effect are significant, we also show the cospectrum between CO_2 and T in Fig. 7. While the cospectrum of the measurements is negative at all time scales, this correlation reverses sign in the 'natural' cospectrum for the mesoscale motion ($\sim$1000 s).

5 Conclusions

We proposed a set of expressions to evaluate the higher-order scalar density statistics measured by open-path gas analyzers when they are linked to turbulent transport processes in the atmosphere. Similarly to the vertical flux corrections, we showed that both higher-order turbulent moments such as the scalar variance, the mixed velocity-scalar covariance, and the two-scalar covariance require adjustments—and these adjustments can be formally expressed as a function of temperature and water vapour fluctuations. We also showed that the impact of these adjustments on dimensionless similarity functions derived from flux-variance relationships is significant. Both the PDF and the spectra of the CO_2 are significantly modified by these adjustments. Finally, given the large corrections in the spectra and PDF, it is only logical to employ Eq. 5 directly on the high-frequency time series prior to micrometeorological data analysis.

Acknowledgements We thank P. Stoy, J.Y. Juang, and M.B. Siqueira for their help in setting up the experiment, and M. Mancini for his overall support. Funding for the data was provided by the Biological and Environmental Research (BER) Program, US Department of Energy, through their Terrestrial Carbon Processes, and through the Southeast Regional Center (SERC) of the National Institute for Global Environmental Change (NIGEC).

References

Aubinet M, Berbigier P, Bernhofer CH, Cescatti A, Feigenwinter C, Granier A, Grunwald TH, Havrankova K, Heinesch B, Longdoz B, Marcolla B, Montagnani L, Sedlak P (2005) Comparing CO_2 storage and advection conditions at night at different carboeuroflux sites. Boundary-Layer Meteorol 116:63–94

Baldocchi D, Falge E, Gu LH, Olson R, Hollinger D, Running S, Anthoni P, Bernhofer C, Davis K, Evans R, Fuentes J, Goldstein A, Katul G, Law B, Lee XH, Malhi Y, Meyers T, Munger W, Oechel W, U KTP, Pilegaard K, Schmid HP, Valentini R, Verma S, Vesala T, Wilson K, Wofsy S (2001) FLUXNET: a new tool to study the temporal and spatial variability of ecosystem-scale carbon dioxide, water vapor, and energy flux densities. Bull Am Meteorol Soc 82:2415–2434

Choi TJ, Hong JY, Kim J, Lee HC, Asanuma J, Ishikawa H, Tsukamoto O, Gao ZQ, Ma YM, Ueno K, Wang JM, Koike T, Yasunari T (2004) Turbulent exchange of heat, water vapor, and momentum over a Tibetan prairie by eddy covariance and flux variance measurements. J Geophys Res Atmos 109:D21106 doi:10.1029/2004JD004767

de Arellano JVG, Gioli B, Miglietta F, Jonker HJJ, Baltink HK, Hutjes RWA, Holtslag AAM (2004) Entrainment process of carbon dioxide in the atmospheric boundary layer. J Geophys Res Atmos 109:D18110, doi:10.1029/2004JD004725

Feigenwinter C, Bernhofer C, Vogt R (2004) The influence of advection on the short term CO2-budget in and above a forest canopy. Boundary-Layer Meteorol 113:201–224

Fuehrer PL, Friehe CA (2002) Flux corrections revisited. Boundary-Layer Meteorol 102:415–457

Juang J-Y, Katul GG, Siqueira MB, Stoy PC, Palmroth S, McCarthy HR, Kim HS, Oren R (2006) Modeling nighttime ecosystem respiration from measured CO_2 concentration and air temperature profiles using inverse methods, J Geophys Res Atmos 111, D08S05, doi:10.1029/2005JD005976

Katul GG, Geron CD, Hsieh CI, Vidakovic B, Guenther AB (1998) Active turbulence and scalar transport near the land-atmosphere interface. J Appl Meteorol 37:1533–1546

Katul GG, Goltz SM, Hsieh CI, Cheng Y, Mowry F, Sigmon J (1995) Estimation of surface heat and momentum fluxes using the flux-variance method above uniform and non-uniform terrain. Boundary-Layer Meteorol 74:237–260

Liebethal C, Foken T (2003) On the significance of the Webb correction to fluxes. Boundary-Layer Meteorol 109:99–106

Liu HP (2005) An alternative approach for CO_2 flux correction caused by heat and water vapour transfer. Boundary-Layer Meteorol 115:151–168

Massman WJ, Lee X (2002) Eddy covariance flux corrections and uncertainties in long-term studies of carbon and energy exchanges. Agric Forest Meteorol 113:121–144

Moriwaki R, Kanda M (2004) Seasonal and diurnal fluxes of radiation, heat, water vapor, and carbon dioxide over a suburban area. J Appl Meteorol 43(11):1700–1710

Novick KA, Stoy PC, Katul GG, Ellsworth DS, Siqueira MBS, Juang J, Oren R (2004) Carbon dioxide and water vapor exchange in a warm temperate grassland. Oecologia 138:259–274

Scanlon TM, Albertson JD (2001) Turbulent transport of carbon dioxide and water vapor within a vegetation canopy during unstable conditions: Identification of episodes using wavelet analysis. J Geophys Res Atmos 106:7251–7262

Siqueira M, Lai CT, Katul G (2000) Estimating scalar sources, sinks, and fluxes in a forest canopy using Lagrangian, Eulerian, and hybrid inverse models. J Geophys Res Atmos 105:29475–29488

Staebler RM, Fitzjarrald DR (2004) Observing subcanopy CO_2 advection. Agric Forest Meteorol 122:139–156

Webb EK, Pearman GI, Leuning R (1980) Correction of flux measurements for density effects due to heat and water-vapor transfer. Quart J Roy Meteorol Soc 106:85–100